

Numerical modelling of cantilever failure and effect of slump blocks on meander migration

Kattia Rubi Arnez Ferrel^{1,*}, *Ichiro Kimura*², and *Yasuyuki Shimizu*³

¹Graduate School of Engineering, Hokkaido University, Japan

²University of Toyama, Japan

³Graduate School of Engineering, Hokkaido University, Japan

Abstract. This study proposes a new numerical model to study cantilever failures and the effect of slump blocks on meander migration in cohesive river banks. Previous models have incorporated the effect of slump blocks using different methodologies but most of them used an “indirect approach” (such as increasing the critical shear stresses or introducing armouring factors) which does not allow to evaluate the effect of slump blocks directly. The new numerical model introduces an explicit representation of slump blocks and it was obtained by coupling two models available on the literature. The model was able to represent the mechanisms of cantilever failure with slump blocks and their effect in meander migration in a hypothetical small scale channel.

1. Introduction

Meanders in rivers are among the most beautiful patterns that we can observe in nature. These meandering patterns are found all around the world and they are characterized for having one single channel with a sinusoidal shape, where the water flows in a succession of opposite bends [1]. Many researchers have studied meanders [1-5], especially in the last five decades.

Regardless the effort of understanding these complicated systems, the reason why the meanders "migrate" the way they do is still not well understood.

Two major processes in meander migration are bank erosion and bank accretion [1]. Bank erosion is considered a major hazard all over the world. It is unpredictable and has severe social, economic and environmental impact. As a result of bank migration, the loss of soil eventually will threat structures established near riverbanks as well as human lives.

In this study, we focused on cantilever failures which are characterized by the development of an overhanging part as a result of fluvial erosion in banks with cohesive material. The overhanging part eventually falls into the water and it remains in front of the bank until erosion occurs again. This chunk called “a slump block” mostly protects the bank and as a result migration rates decrease [4]. The objective of this paper is to develop a numerical model to study the effect of slump blocks in the meander river migration.

* Corresponding author: rubikraf@gmail.com

Given the large temporal and spatial scale in rivers, we considered that the best approach for this problem was to develop a numerical model. Although there are plenty of models for modelling bank erosion, very few include the effect of slump blocks explicitly [3-5].

We selected the bank erosion model developed by Patsinghasanee et al [6-7], which was developed to study cantilever failures in a straight flume. To our knowledge, this model is one of the first in explicitly including the effect of slump blocks in the bank geometry as well as the decomposition process of slump blocks.

As it was explained, it is required to take into account the streamwise variation of the curvature in order to simulate meander migration. From all the literature reviewed, we considered the flow model of Garcia et al. [2] best fits to our methodology.

Other improvements of the model such as bank accretion and effect of secondary flow of the first kind are also considered in this model and they are described in the methodology section.

2. Methodology

The model proposed in this paper is the result of the merging of two models: Patsinghasanee et al and Garcia's et al solution. Other improvements are explained in this section.

2.1. Flow model (Garcia et al model)

The hydrodynamic model of Garcia et al [2] is based on the two-dimensional St. Venant depth-averaged equations and the depth-averaged continuity equation.

Assuming a constant width and a linear transverse bed elevation in function of the curvature, a mathematical solution was found for the near-bank perturbation velocity u_b :

$$u_b(s) = a_1 e^{-a_2 s} + a_3 C(s) + a_4 e^{-a_2 s} \int_0^s C(s) e^{a_2 s} ds \quad (1a)$$

$$a_1 = u(0) + \chi C(0) \quad (1b)$$

$$a_2 = 2C_{f0} \beta \chi \quad (1c)$$

$$a_3 = -\chi \quad (1d)$$

$$a_4 = C_{f0} \beta [\chi^5 F_0^2 + (\alpha + 1) \chi^2 + 5\sqrt{C_{f0}} \chi^2 (\alpha + \chi^3 F_0^2)] \quad (1e)$$

$$\chi = \left(\frac{S_0}{S_v} \right)^{1/3} \quad (1f)$$

where $\beta = B^*/D_o$, B^* is the channel half-width, C is the channel curvature, α is a constant coefficient that controls the steepness of the transverse slope of the channel bed, S_0 is the averaged meandering channel slope, D_o is the reach-averaged water depth, S_v represents the valley slope and F_0 denotes the Froude number. The friction coefficient C_{f0} can be calculated as:

$$C_{f0} = 6 + 2.5 \ln \left(\frac{D^*}{2.5 d_s^*} \right)^{1/3} \quad (2)$$

where d_s^* is a measure of the bed grain size and D^* is the local flow depth. A more detailed description can be found in the original paper.

2.2. Bank erosion model (Patsinghasanee et al.)

The cantilever failure and the different stages that describe the phenomenon are taken into account in this model. The authors [5] observed in their experiments that the phenomenon of

cantilever failures followed four stages: fluvial erosion, development of tension cracks, failure of overhanging part and falling of bank material in the bed channel and, slump blocks decomposition and sediment transport of the banks [5].

Based on these observations, the authors conceptualized the problem and developed a cross sectional model to represent the bank erosion in rivers with cohesive banks. The model used a triple grid approach, considering a coarse one-dimensional (1-D) grid for the flow calculations in the lateral direction, a fine 1-D grid for the sediment transport and bed deformation in the lateral direction and a 2-D fine grid for computation of the soil.

The fluvial erosion in the model was calculated using the well know equation of Partheniades (1965), that relates the rate of bank erosion with the excess shear stress formula given below:

$$\varepsilon = k_d (\tau_{b0} - \tau_{bc})^a \tag{3}$$

where ε is the fluvial erosion rate of the bank (m/s), k_d is the erodibility coefficient ($\text{m}^3/(\text{N s})$), τ_{b0} is the actual shear stress applied by the flow (Pa), τ_{bc} is the critical shear stress of the bank (Pa) and a is an exponent generally assumed to be equal to one. The actual shear stress was calculated in each cell using the following equation:

$$\tau_{b0} = \rho g R_j i \tag{4}$$

where R_j is the hydraulic radius in each calculation cell (A_j/P_j), A_j is the cross-sectional area of a cell, P_j is the wetted perimeter of a cell, j is the lateral cell number and i is the energy slope. In the model, uniform flow conditions were assumed and therefore, the energy slope was set equal to the bed slope. The velocity in each cell u_j was calculated using Manning’s formula:

$$u_j = \frac{1}{n_m} R_j^{2/3} i^{1/2} \tag{5}$$

where n_m is the Manning roughness parameter along the channel calculated using the Manning-Strickler equation ($k_s^{1/6}/7.66g^{1/2}$) and k_s is the roughness height defined as $1.5d_{50}$. For the next stage, the cantilever failure was analysed using a limit equilibrium analysis. Two types of failure were considered: shear and beam failures (Fig. 1).

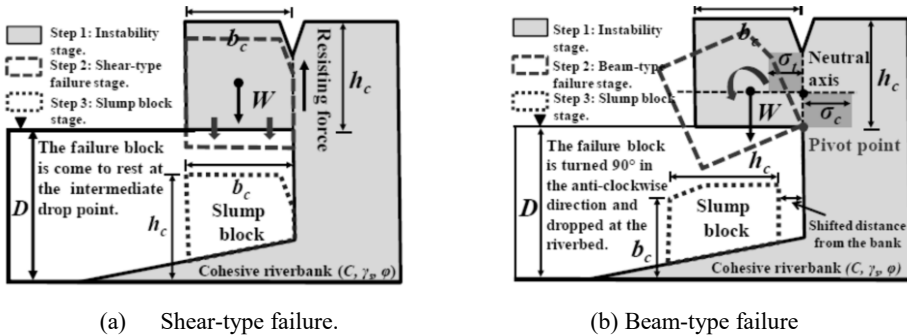


Fig. 1. Cantilever failure mechanisms [5].

Shear failure occurs when the shear stress along the vertical plane of the overhanging block weight exceeds the resistance force of the cohesive bank [5] as shown in Fig. 1a. As a consequence, the slump block falls directly into the water maintaining its initial dimensions.

On the other hand, the beam failure takes place when the rotational moment of the overhanging block overcomes the resistive moments of the soil strengths in the tension and compression zone [5] as illustrated in Fig. 1b. The overhanging block falls into the water rotating 90 degrees from the pivot point which is located at the lowest edge of the failure plane.

The criteria used to determine whether shear or beam failure will occur depend on the safety factor with the smaller value. Once the failure occurs, the material is deposited in the riverbed in front of the banks and the decomposition process begins. Slump blocks are decomposed by fluvial erosion in two different materials: sand and silt. The silt is assumed to become wash load, and the failed sand acts as bedload. An important assumption of this model is considering that the strength of the slump block is reduced once it falls into the riverbed, because the slump block experienced a disturbance due to the dropping [5] and therefore the fluvial erosion for slump blocks is calculated as follows:

$$\varepsilon_{sb} = k_{sb} \varepsilon \quad (6)$$

where ε_{sb} is the fluvial erosion rate of the slump block (m/s) and k_{sb} is the coefficient of the fluvial erosion rate. This coefficient of fluvial erosion rate is calculated by trial and error in order to get the best agreement with the experimental results [6]. However in this paper, we consider the value of k_d equal to 1.2 similar to the experimental value of [6].

In the program we can select between the equation of Meyer-Peter Muller (1948) and the Ashida and Michiue (1972). In this paper the equation of Ashida and Michie (1972) was selected:

$$q_{bs} = 17 \tau_*^{\frac{3}{2}} \left(1 - \frac{\tau_c^*}{\tau_*}\right) \left(1 - \sqrt{\frac{\tau_c^*}{\tau_*}}\right) \sqrt{s_g g D_{50}^3} \quad (7)$$

where τ^* is the non-dimensional bed shear stress and τ_c^* is the non-dimensional critical bed shear stress (Iwagaki's equation, 1956), s_g is the specific weight of sediment (2.65), and g is gravity acceleration (9.81 ms⁻²).

In the model of Patsinghasanee et al, the sediment transport rate in the lateral direction q_{bn} was evaluated using the Hasegawa's equation, neglecting the secondary current of first kind because a straight channel was considered, as given:

$$q_{bn} = -q_{bs} \sqrt{\frac{\tau_c^*}{\mu_s \mu_k \tau_*}} \frac{\partial z_b}{\partial y} \quad (8)$$

where z_b is the bed elevation; μ_s and μ_k are the static (=1.0) and dynamic (=0.45) friction factors and y is the coordinate component in the lateral direction.

The bed deformation was calculated using a continuity equation of the bed as:

$$\frac{\partial z_b}{\partial t} + \frac{1}{1-\lambda} \left(\frac{\partial q_{bn}}{\partial y} \right) = 0 \quad (9)$$

where t is time and λ is the porosity of the material (=0.4).

2.3. Coupling of the flow and bank erosion model

The coupling process between the two models is considered by correcting the velocity profile of Patsinghasanee et al using the near-bank velocity equation derived by Garcia et al's model.

A weight function which depends on the near bank velocity is calculated using the near-bank velocity equations as follows:

$$u_{c_j} = u_j (1 + u_b n_j) \quad (10)$$

where u_{c_j} are the corrected velocities and u_j are the velocities obtained from Equation (5) and n_j is the non-dimensional coordinate in lateral direction defined as $n_j = n_j^* / B^*$.

Equation (10) allows us to obtain a more realistic profile where the higher velocities are obtained in the outer bank of the bends.

2.3.1. Migration of the centreline

The migration of the channel centreline is calculated similarly as in [5]. First, the width of the channel in each section is calculated after every time step and then the coordinates of the left and right banks are obtained. The left and right bank coordinates correspond to the point where the water intersects with the bank. The coordinate of the centre of the channel (nc) can be calculated. Then, the shifted distance from the current centre of the channel (nc_{new}) to the previous one (nc_{old}) along the cross section is calculated as follows:

$$\Delta n = nc_{new} - nc_{old} \tag{11}$$

The inclination θ of each cross-section with respect to x axis is considered and finally the coordinates of the new channel centreline are calculated with equations (12 a-b). The procedure is represented in Fig. 2.

$$xc_{new}(i) = xc_{old}(i) - \Delta n * \sin \theta \tag{12a}$$

$$yc_{new}(i) = yc_{old}(i) + \Delta n * \cos \theta \tag{12b}$$

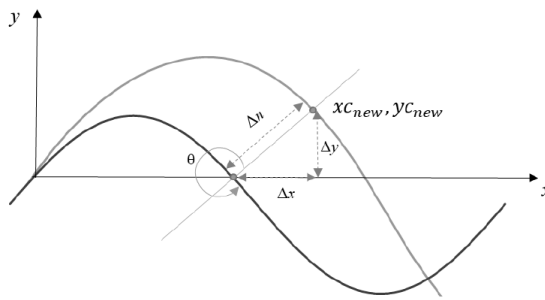


Fig. 2. Schematic representation of the centreline migration.

The curvature C is calculated using Eq. (13) and the first and second derivatives are evaluated using a central difference scheme.

$$C = \frac{\frac{d^2 y}{dx^2}}{\left(1 + \left(\frac{dy}{dx}\right)^2\right)^{3/2}} \tag{13}$$

2.4. Model Refinement

We consider the effect of the secondary flow of the first kind in the equation of the sediment transport rate in the lateral direction (Eq. 8) as follows:

$$q_{bn} = \frac{u_{bn}}{u_{bs}} - q_{bs} \sqrt{\frac{\tau_c^*}{\mu_s \mu_k \tau_*}} \frac{\partial z_b}{\partial y} \tag{14a}$$

$$u_{bn} = -N_* \frac{D^*}{r} u_{bs} \tag{14b}$$

where u_{bs} and u_{bn} are the near-bed velocities in streamwise and transverse directions and N^* is the coefficient of the strength of secondary flow (assumed to be 7.0 for simplicity).

In addition, a sub model for simulating bank accretion was considered. We took into account a critical time (T_{cr}) for the bank to grow based the critical shear stress and a minimum depth (10% of the initial depth h_0) condition. If the value of the model remains under that condition for a time longer than the critical time then bank accretion occur. This approach is based on the model of Asahi et al [8].

$$\begin{aligned} \text{If } \tau < \tau_c \text{ or } h < 0.1h_0 \text{ then } T=T+\Delta T \quad \text{else } T=0 \\ \text{If } T > T_{cr} \text{ then bank erosion occurs.} \end{aligned}$$

Finally, as it was observed by other researchers [1, 5] this kind of methodology leads to developing of oscillations in the curvature. In order guarantee continuity between sections, we included Parametric Cubic Splines interpolations (PCS).

3. Model application

3.1. Case: One sinusoidal bend

For this case a hypothetical channel with similar characteristics to the experimental data of Patsinghasanee et al. (2017) is considered.

The initial form of bend in the channel is generated by the sine-generated curve equation:

$$\theta = \theta_0 \sin\left(\frac{2\pi s}{L}\right) \tag{15}$$

where θ is the angle that path makes with the horizontal at a given point, θ_0 is the maximum angle that the curve makes with the horizontal, L is the length of the channel centreline over one meander length and s is the distance along the length of the channel.

The channel is composed of a rectangular cross-section channel with a width of 0.3 m, bank height of 0.2 m and a total length of 28 m. The initial plan shape consists of a straight channel of 4 m, one sinuous section of 8 m and again a straight channel with a length of 16 m. The sinuous part of the channel is generated with equation (17) with an initial meander angle $\theta_0=20^\circ$. The channel in total is composed of 71 nodes as shown in the following figure.

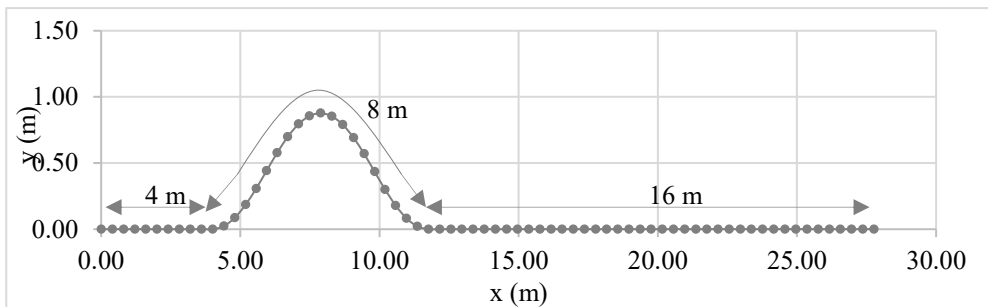


Fig. 3. Top view of the initial channel centreline.

The initial conditions used for the calculations are shown in table 1. In the experiments of Patsinghasanee et al. (2017) the sediment mixture is composed of sand and silt with a diameter of 0.23 mm and 28.4 μ m respectively. Two cases were simulated, the first case considering the effect of slump blocks and the second case neglecting the effect of slump blocks. This means that Case 2 considers the effect of correction in the velocity profile and secondary flow effect only, assuming that once the material has fallen into the river is just transported as wash load. The results of the simulations are shown in Fig. 4 and 5 respectively

Table 1. Variables used in the simulation.

Discharge	Bank height	Channel width	Silt clay content	Slope	Manning coefficient	Critical shear stress	Mean diameter
Q	h	w	SC	i	n_m	τ_c	D_{50}
L/s	m	m	%	-	$m^{-1/3}/s$	Pa	mm
6.45	0.20	0.3	30	0.001	0.011	0.61	0.23

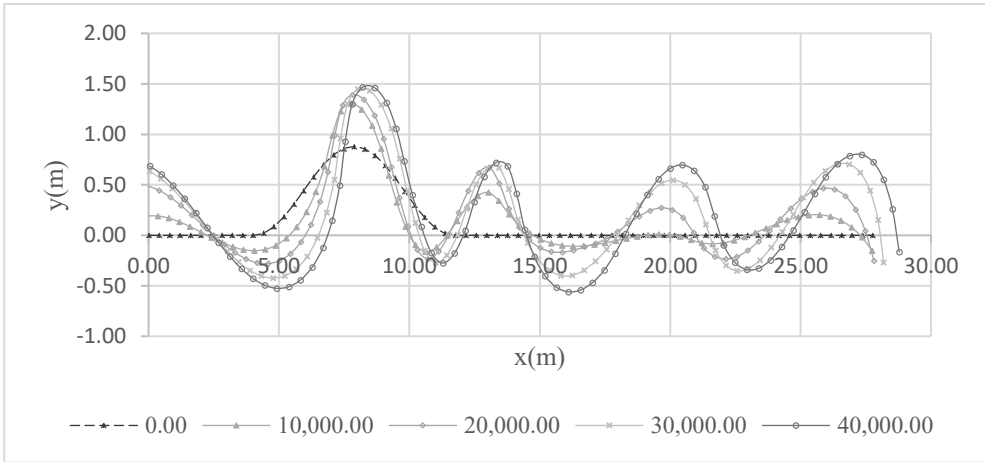


Fig. 4. Migration of the channel centreline for Case 1 (Including the effect of slump blocks)

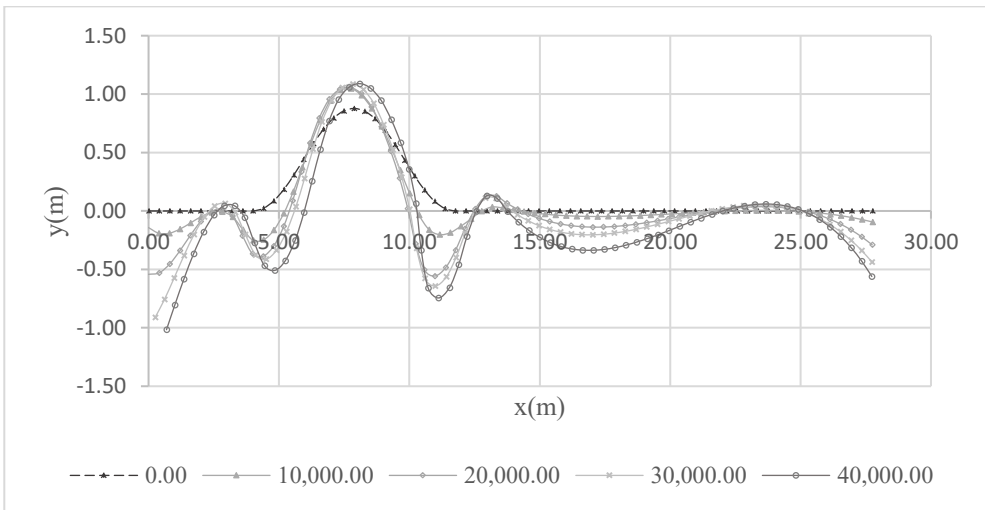


Fig. 5. Migration of the channel centreline for Case 2 (Neglecting effect of slump blocks).

In both cases we considered the same computational conditions. We run the simulations for 40000 (s) and the results are plotted every 10000 (s). In addition, the initial and final point of the channel were not fixed.

For Case 1 (Fig. 4) we can see initial bend increases its amplitude in the sections corresponding to the apex from 0.90 to 1.46 m. The length of the channel increases from 28 m at the beginning to 32 m at the end of the simulation. Downstream, three small meanders

with wavelengths of 4.82m, 6.83m and 5.85m are formed. The initial angle of meandering increases, giving the bend that “pointy” form. The meander migrates downstream.

On the other hand, Case 2 (Fig 5) shows the development of one meander bend downstream. The amplitude of the initial bend is smaller than in Case 1 (1.06 m). The meander migrates towards downstream. One small meander is developed downstream with an amplitude that remains constant in time.

4. Conclusions

The effect of slump blocks in a small scale meandering channel was studied by means of numerical modelling.

A new coupled model was developed to reach this objective with the following special features: 1) the velocity profile was corrected by a weight function that depends on the near-bank velocity; 2) the effect of secondary flow was considered in the Hasegawa’s equation for lateral sediment transport; 3) variation in the downstream curvature and 4) bank accretion was considered. The model was applied to two cases: the first one including the effect of slump blocks and the second one neglecting the effect of slumps blocks. The results showed that slump blocks change the plan shape of the channel.

As pointed out by Kleinhans et al., “both processes bar and bend instabilities play important roles in the evolution of the meandering channels and thus should be incorporated into the analysis of the evolution of meandering” [9]. As this model cannot reproduce bed forms, the effect shown on this paper results from the variation of the radius of curvature only. More study is necessary to confirm this conclusion.

The authors want to acknowledge to the Japanese Government Scholarship (MEXT) for providing financial support.

References

1. A. Crosato, *Analysis and modelling of river meandering* PHD Thesis, (2008)
2. M. Garcia, L. Bittner, Y. Nino, , *Mathematical modelling of meandering streams in Illinois: A tool for stream management and engineering* Univ. of Illinois at Urbana-Champaign (1996)
3. D. Motta, D. Abad, J. Langendoen and M. Garcia, *J. Geomorphology A simplified 2D model for meander migration with physically-based bank evolution*, 163-164, (2012)
4. D. Motta, E. J. Langendoen, J.D. Abad, M. H. Garcia, *Modification of meander migration by bank failures*, *J. Geophys. Res. Earth Surf* **119**, 1026-1042 (2014)
5. D. Motta, *Meander migration with physically-based bank erosion*, PHD Thesis, Univ. Illinois at Urbana-Champaign (2013)
6. S. Patsinghasanee, I. Kimura, Y. Shimizu, *Numerical simulation of a cantilever failure with the effect of slump blocks for cohesive riverbanks*, *J. Hydraulic Eng. JSCE* **72**, 493-498 (2016)
7. S. Patsinghasanee, I. Kimura, Y. Shimizu, M. Nabi, *Experiments and modelling of cantilever failures for cohesive riverbanks*, *J. Hydraulic Research. JSCE* **72**, 493-498, (2017)
8. K. Asahi, Y. Shimizu, J. Nelson, G. Parker, *Numerical simulation of river meandering with self-evolving banks*, *J. Geophys. Res. Earth Surf* **118**, 2208-2229 (2013)
9. M. Kleinhans, H. van den Berg, *River channel and bar patterns explained and predicted by an empirical and physics-based method*, *Earth Surf. Process. Landforms* **36**, 721-738 (2011)